JOURNAL OF INTEGRATED OMICS
A METHODOLOGICAL JOURNAL
HTTP://WWW.JIOMICS.COM

ORIGINAL ARTICLE | DOI: 10.5584/jiomics.v9i1.273

Molecular mechanisms of adaptation to the habitat depth in visual pigments of *A. subulata* and *L. forbesi* squids: on the role of the S270F substitution

Dmitrii M. Nikolaev [1], Demid E. Osipov [2], Daniil M. Strashkov [1], Sergey Yu. Vyazmin [1], Vasily E. Akulov [1], Denis V. Kravtcov [3], Oleg B. Chakchir [1], Maxim S. Panov [3], Mikhail N. Ryazantsev [3*]

[1] Department Nanotechnology Research and Education Centre RAS, Saint-Petersburg Academic University, 8/3 Khlopina Street, St. Petersburg 194021, Russia; [2] Peter the Great St. Petersburg Polytechnic University, Polytekhnicheskaya Str. 29, St. Petersburg, 195251, Russia; [3] St. Petersburg State University, Institute of Chemistry, Universitetskiy Ave. 26, St. Petersburg, Petergof, 198504, Russia

Received: 09 January 2019 **Accepted:** 03 May 2019 **Available Online**: 27 June 2019

Abstract

Revealing the mechanisms of animal adaptation to different habitats is one of the central tasks of evolutionary physiology. A particular case of such adaptation is the visual adaptation of marine species to different depth ranges. Because water absorbs more intensively longer wavelengths than shorter wavelengths, the increase of habitat depth shifts the visual perception of marine species towards the blue region. In this study, we investigated the molecular mechanisms of such visual adaptation for two squid species – *Alloteuthis subulata* and *Loligo forbesi*. These species live at different depths (200 m and 360 m, respectively) and the absorption maximum of *A. subulata* visual rhodopsin is slightly red-shifted compared to *L. forbesi* rhodopsin (499 and 494 nm, respectively). Previously, the amino acid sequences of these two species were found to differ in 22 sites with only seven of them being non-neutral substitutions, and the S270F substitution was proposed as a possible candidate responsible for the spectral shift. In this study, we constructed computational models of visual rhodopsins of these two squid species and determined the main factors that cause the 5 nm spectral shift between the two proteins. We find that the origin of this spectral shift is a consequence of a complex reorganization of the protein caused by at least two mutations including S270F. Moreover, the direct electrostatic effect of polar hydroxyl-bearing serine that replaces non-polar phenylalanine is negligible due to the relatively long distance to the chromophore.

Аннотация

Определение механизмов адаптации животных к различным условиям среды является одной из центральных задач эволюционной физиологии. Частным случаем такой адаптации является зрительная адаптация морских животных к различным глубинам. Так как вода поглощает длинноволной свет более интенсивно, чем коротковолновой, то с увеличением глубины обитания происходит сдвиг видимой части спектра морских животных в синюю область. В данном исследовании мы изучили молекулярные механизмы, обеспечивающие зрительную адаптацию двух кальмаров — *Alloteuthis subulata* и *Loligo forbesi*. Эти кальмары живут на разных глубинах (200 м и 360 м соответственно), и максимум поглощения зрительного родопсина *A. subulata* слегка сдвинут в длинноволновую область относительно родопсина *L. forbesi* (499 и 494 нм соответственно). В более ранней работе уже проводился анализ аминокислотных последовательностей этих двух видов, который показал наличие 22 аминокислотных замен, только семь из которых были неконсервативными. Было выдвинуто предположение, что аминокислотная замена S270F является возможной причиной наблюдаемого спектрального сдвига. В данной работе мы сгенерировали компьютерные модели визуальных родопсинов двух кальмаров и определили основные факторы, которые отвечают за 5 нм спектральный сдвиг между белками. Мы обнаружили, что причиной спектрального сдвига является сложная реорганизация белка, вызванная как минимум двумя мутациями, включая S270F. Более того, мы показали, что прямой электростатический эффект полярного серина, который заменяется неполярным фениланином, незначителен, так как данная аминокислота находится на значительном расстоянии от хромофорора.

Keywords: Visual adaptation; squid rhodopsins; molecular mechanisms of visual adaptation; *L. forbesi* vision; *A. subulata* vision; non-direct tuning in rhodopsins; spectral tuning in rhodopsins

***Corresponding author:** Mikhail N. Ryazantsev, candidate of chemical sciences, associate professor of Saint-Petersburg State University, Institute of Chemistry, Universitetskiy Ave. 26, St. Petersburg, Petergof, 198504, Russia.

1. Introduction

Understanding the molecular mechanisms of visual adaptation is an essential problem of evolutionary physiology that allows for deriving general patterns of rhodopsin alterations during the evolution of vision. A prime example is the visual adaptation of marine species to the habitat depth. An increase of habitat depth correlates with a blue-shifting of visual range of marine animals, which can be rationalized by the fact that longer wavelengths are more intensively absorbed by water. For example, the rod pigments of a majority of deep-sea fish exhibit λ_{max} around 480 nm close to the maximum of oceanic water light transmission. A similar blue shift has been found both in the rod and cone pigments of cottoid fish species that live in fresh-water Lake Baikal, in visual pigments of rockfishes and crustacean.[1-3]

In this study, we consider a particular case of such visual adaptation by comparing the visual rhodopsins of two squid species. While *Alloteuthis subulata* squid lives at the depth range around 200 m and its rhodopsin demonstrates an absorption maximum at 499 nm, *Loligo forbesi* lives at the depth around 360 m and the absorption maximum value of its rhodopsin is 494 nm. The origin of this shift has already been studied experimentally.[4] According to this study, the amino acid sequences of these two rhodopsins differ only in 22 sites, and only seven of them are non-neutral substitutions. The substitution S270F was attributed as a possible candidate responsible for the 5 nm difference. The S270F substitution was singled out as a reasonable candidate because it is the only substitution of a polar hydroxyl-bearing serine located relatively close to the chromophore with the non-polar phenylalanine. In this study, we constructed a series of computational Quantum Mechanics/ Molecular Mechanics (QM/MM) models for rhodopsins of *A. subulata* and *L. forbesi* and their mutants.

We found that direct electrostatic effect of the S270F substitution cannot lead to any spectral shift due to the relatively long distance from the chromophore. However, the S270F substitution, along with other substitutions, is responsible for the significant reorganization of the hydrogen bond network in the protein that leads to change in the position of the polar and charged residues including the counterion E180. Thus, the spectral shift between *A. subulata* and *L. forbesi* rhodopsins is an example of complex non-direct spectral tuning rather than a direct electrostatic effect of substituted residues. In addition, the spectral shift between *A. subulata* and *L. forbesi* rhodopsins cannot be explained completely by a single S270F substitution, and other non-neutral substitutions are involved in the tuning of the spectral shift.

2. Material and Methods

The structures of *A. subulata* and *L. forbesi* visual rhodopsins were generated using a homology modeling approach on the basis of their primary sequences (UniProt codes Q17094 and P24603, respectively).[4, 5] The X-ray structure of *Todarodes Pacificus* visual rhodopsin (RCSB code 2Z73) was used as a template.[6] To align primary sequences we used AlignMe program package.[7] The obtained values of sequence identity between target proteins and the template (83% and 85% for *A. subulata* and *L. forbesi*, respectively) were very high, i.e. the structures of all three proteins are very similar. To generate the three-dimensional structures of target rhodopsins we applied the I -TASSER program package.[8] Because I-TASSER can generate several structures based on its scoring functions and does not take into consideration the membrane environment, we used visual inspection to sort out the structure(s) with the correct fold. For each of the studied rhodopsins and mutants, all structures except a single one folded incorrectly, i.e. they could not exist in the membrane environment. The final structures were subjected to additional processing and optimization. We inserted the retinal chromophore in rhodopsin models bound to the K305 residue. Proteins were hydrated with Dowser++ program.[9] Then we used pdb2pqr (version 2.1.1)[10] and propka (version 3.0)[11] programs to calculate pKa values for the titratable amino acids in proteins, assign their protonation states (pH=7.0) and add hydrogen atoms. These complete models were subjected to geometry optimization first at the MM level (AMBER force field)[12] and then applying a hybrid quantum-mechanics/molecular-mechanics approach [QM:MM (SORCI+Q//B3LYP/6-31g (d):AMBER-96)] implemented in Gaussian09 program package.[13] To calculate absorption maxima values of the retinal chromophore in protein environment we applied SORCI+Q/6-31G* level of theory implemented in ORCA 4.0 program package.[14] The same methodology was applied to perform all other spectral calculations performed in the current work. All applied protocols have been successfully tested in a number of previous studies.[15-24]

For both proteins amino acid numbering is in accordance with the published *L. forbesi* amino acid sequence.[5] .

3. Results

The absorption maxima values calculated for the generated three-dimensional rhodopsin models were in good agreement with experimental values and reproduced the experimentally observed spectral red shift of *A. subulata*

Table 1 | The comparison of calculated and experimental absorption wavelengths of rhodopsins from *A. subulata* and *L. forbesi.*
Сравнение рассчитанных и экспериментальных значений λ_{max} для родопсинов кальмаров *A. subulata* и *L. forbesi.*

	***A. subulata* λ_{max}, nm**	***L. forbesi* λ_{max}, nm**
experimental	499	494
calculated	473	467

Table 2 | Absorption maxima values for several computational models of visual rhodopsins from *A. subulata, L. forbesi, A. subulata* S270F mutant and *L. forbesi* rhodopsin F270S mutant. a) Model 2 is the retinal chromophore with geometry optimized in corresponding protein environment of rhodopsin in the absence of external charges. b) Model 3 is the retinal chromophore in the presence of charges corresponding to the E180 residue, the rest of AMBER charges of protein atoms are set to zero. c) Model 4 is the retinal chromophore in the presence of charges corresponing to the E180 residue, polar residues and water molecules located within 5 Å from the retinal chromophore. d) Model 5 is the model that contains all residues of the protein. Значения λ_{max} для нескольких вычислительных моделей изучаемых белков: зрительных родопсинов кальмаров *A. subulata, L. forbesi*, мутанта родопсина *A. subulata* S270F и мутанта родопсина *L. forbesi* F270S. a) Модель 2 представляет собой ретинальный хромофор, геометрия которого была оптимизирована в соответствующей белковой среде родопсина. b) Модель 3 представляет собой ретинальный хромофор и заряды, соответствующие аминокислоте E180, остальные AMBER заряды на атомах белка приравнены нулю. c) Модель 4 представляет собой ретинальный хромофор и заряды, соответствующие аминокислоте E180, а также полярным аминокислотам и молекулам воды, расположенным в пределах 5 Å от ретинального хромофора. d) Модель 5 представляет собой ретинальный хромофор и заряды всех аминокислот белка.

Model	*A. subulata* λ_{max}, nm	*L. fobesi* λ_{max}, nm	*A. subulata* S270F λ_{max}, nm	*L. forbesi* F270S λ_{max}, nm
Model 2[a]	603	601	596	603
Model 3[b]	525	501	524	532
Model 4[c]	487	467	487	501
Model 5[d]	473	467	476	485
full protein with charges of S270/F270 set to zero	471	465		

rhodopsin relative to *L. forbesi* rhodopsin (Table 1). To analyze the origin of this spectral shift we performed a series of additional calculations for each rhodopsin model (Table 2).

Eq. 1 $$\Delta\lambda_{max}^{A-L} = \lambda_{max}^{A.subulata} - \lambda_{max}^{L.forbesi}$$

To discern the impact of different factors to the 5 nm spectral shift between two proteins (Equation 1), we performed the following analysis (see Figure 1). First, we calculated λ_{max} for the gas-phase chromophore (11-cis protonated Schiff base, PSB11) (Model 1). After that, we evaluated the spectral shift caused by the retinal geometry modification by a protein environment. To accomplish this task, we calculated the absorption maxima of retinal chromophores (with geometries optimized in corresponding protein environments of two rhodopsins) in the absence of external charges (Model 2). These calculations provide the +2 nm absorption red shift of retinal from *A. subulata* rhodopsin compared to retinal from *L. forbesi* rhodopsin.

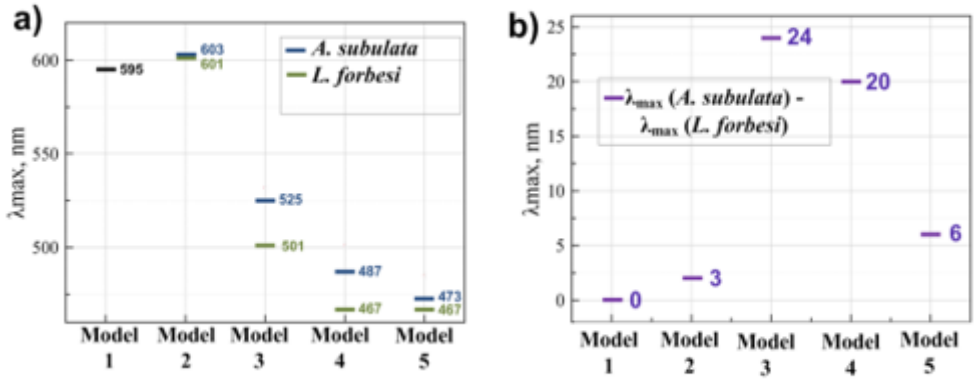

Figure 1 | a) λ_{max} of the investigated computational models of rhodopsins from *A. subulata* (blue) and *L. forbesi* (green). b) The values for the models. Model 1 is the gas-phase chromophore (11-cis protonated Schiff base, PSB11). Model 2 is the retinal chromophore with geometry optimized in corresponding protein environment of rhodopsin in the absence of external charges. Model 3 is the retinal chromophore in the presence of charges corresponding to the E180 residue, the rest of AMBER charges of protein atoms are set to zero. Model 4 is the retinal chromophore in the presence of charges corresponding to the E180 residue, polar residues and water molecules located within 5 Å from the retinal chromophore. Model 5 is the model that contains all residues of the protein. a) Рассчитанные значения λ_{max} для изученных моделей родопсинов *A. subulata* (синий) and *L. forbesi* (зеленый). b) Спектральные сдвиги между моделями. Модель 1 представляет собой хромофор (11-цис протонированное основание Шиффа), геометрия которого была оптимизирована в отсутствии зарядов. Модель 2 представляет собой ретинальный хромофор, геометрия которого была оптимизирована в соответствующей белковой среде родопсина. Модель 3 представляет собой ретинальный хромофор и заряды, соответствующие аминокислоте E180, остальные AMBER заряды на атомах белка приравнены нулю. Модель 4 представляет собой ретинальный хромофор и заряды, соответствующие аминокислоте E180, а также полярным аминокислотам и молекулам воды, расположенным в пределах 5 Å от ретинального хромофора. Модель 5 представляет собой ретинальный хромофор и заряды всех аминокислот белка.

Next, we evaluated the effect of a negatively charged residue located in the retinal-binding pocket (counterion E180). We calculated the absorption maxima of retinal chromophores in the presence of charges corresponding to the E180 residue, setting the rest of AMBER charges of protein atoms to zero (Model 3). The results showed that, in *A. subulata* rhodopsin, the counterion causes a smaller spectral blue shift than in *L. forbesi* rhodopsin (-78 and -100 nm relative to absorption of the retinal model without external charges). Analysis of rhodopsin structure reveals that E180 of *A. subulata* rhodopsin is located further from the NH part of the chromophore than E180 of *L. forbesi* rhodopsin. The distance measured from the closest oxygen atom of E180 to the carbon atom C15 of the chromophore is 6.03 Å vs 3.99 Å for *A. subulata* and *L. forbesi*, respectively (see Figure 2). This trend is in full agreement with previous studies[19,25,26] that state the importance of the counterion distance to NH moiety for spectral tuning. Adding polar residues and water molecules located within 5 Å from the retinal chromophore to the model containing only E180 residue (Model 4) gives the total +20 nm spectral shift of *A. subulata* model relative to *L. forbesi* model. Thus, all residues and water molecules in the retinal-binding pocket except the counterion only slightly decrease the spectral red shift between *A. subulata* and *L. forbesi* rhodopsins caused by the change of the distance from NH moiety to the E180 counterion. In the Figure 3 we show some of the polar residues in the binding pocket with most prominent reorganization. The impact of these residues on λ_{max} is estimated by setting the charges of the corresponding residues to zero. The calculated λ_{max} shifts are given in the Table 3. It worth mentioning that total 4 nm effect for the polar residues reorganization is due to the complex reorganization of many residues, and each of them is responsible for much larger shift than 4 nm. For example, the impact of N87 residue, which is connected to the -N-H part of the chromophore through the hydrogen bond, is -49 nm and -33 nm for *A. subulata* and *L. forbesi* models, respectively. This $\Delta\lambda_{max}$ difference can be explained by the change in the orientation of the $-C(O)NH_2$ part of the N87 residue relative to the –N-H part of the chromophore (see Figure 2 a,b). Another striking example is the reorganization of the –OH part of the S187 residue: due to the change of the dipole moment orientation, the $\Delta\lambda_{max}$ sign changes from positive to negative for *A. subulata* and *L. forbesi* models, respectively. Similarly, a flip of the $-C(O)NH_2$ part of the N185 residue leads to the change of the $\Delta\lambda_{max}$ sign. The above-described effect of polar residues reorganization is also well-known and it has been reported before.[19, 27]

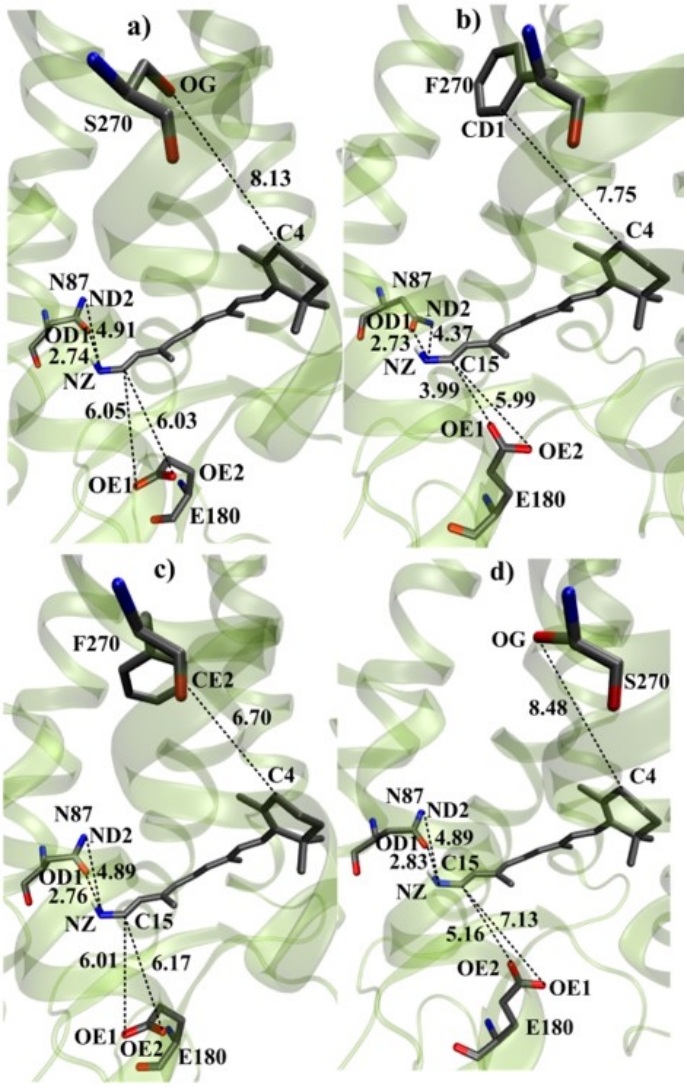

Figure 2 | The comparison of structural differences between four investigated proteins: visual rhodopsins from *A. subulata* (a), *L. forbesi* (b), *A. subulata* rhodopsin S270F mutant(c) and *L. forbesi* rhodopsin F270S mutant (d). All distances are given in Å. Сравнение структур четырех изученных моделей белков: зрительного родопсина *A. subulata* (a), *L. forbesi* (b), мутанта *A. subulata* S270F (c) и мутанта *L. forbesi* F270S (d). Все расстояния приведены в Å.

Table 3 | The impact of polar residues in the retinal-binding cavity of *A. subulata* and *L. forbesi* rhodopsins that show the most prominent reorganization (see Figure 3) on λ_{max}. The effect was estimated by setting the charges of the corresponding residues to zero. Эффект полярных аминокислот в хромофорной полости родопсинов из *A. subulata* и *L. forbesi*, которые демонстрируют наиболее сильную реорганизацию (см. Рисунок 3), на значения λmax. Для расчета эффекта заряды, соответствующие целевой аминокислоте, были приравнены нулю.

Residue	A. subulata $\Delta\lambda_{max}$, nm	L. forbesi $\Delta\lambda_{max}$,
N87	-49	-33
N185	-19	13
C186	-16	-7
S187	16	-12
Y190	17	6

Eq. 2 $$\Delta\lambda_{max}^{A-L}$$

The Model 5 is the model that contains all residues of the

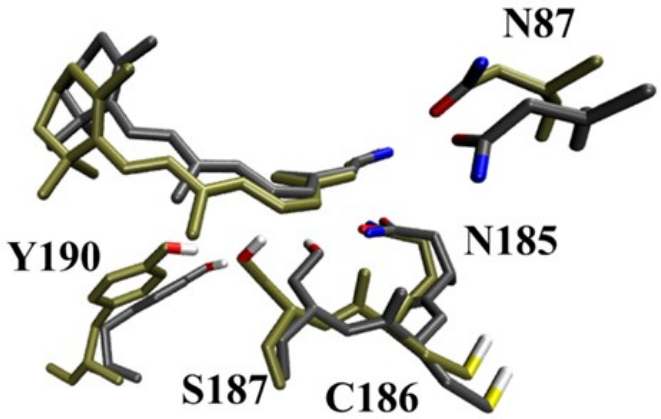

Figure 3 | Polar residues in the binding pocket of A. *subulata* (tan) and *L. forbesi* (gray) rhodopsins that demonstrate the most prominent reorganization. Наиболее сильно реорганизованные полярные аминокислоты в хромофорной полости родопсинов *A. subulata* (желто-коричневый) and *L. forbesi* (серый).

protein. The difference in the (Equation 2) values between models containing the 5 Å cavity and the complete protein models (i.e. -14 nm) can be explained by the reorganization of the charged residues outside the binding pocket.

We also tested the hypothesis proposed in a previous experimental study[4] that the spectral shift is caused by S270F substitution. First, we analyzed the direct electrostatic effect of S270 and F270 residues on the absorption maximum value of retinal chromophore in *A. subulata* and *L. forbesi* rhodopsins, respectively. To perform this task, we constructed new models by setting to zero charges of S270 and F270 in our models of *A. subulata* and *L. forbesi* rhodopsins, and recalculated the absorption maxima without preliminary geometry optimization. The results are given in Table 2. One can see that the above-described elimination of charges does not lead to any change of (Equation 2) value. Moreover, the charges on these residues have a negligible effect on the absorption maxima of the corresponding rhodopsins. The analysis of the predicted rhodopsin structures showed that S270 and F270 residues are located too far from the retinal chromophore (8.13 Å and 7.75 Å, see Figure 2 a,b) to produce a detectable direct electrostatic effect.

As the next step, we investigated if the F270S substitution in *L. forbesi* rhodopsin or S270F substitution in *A. subulata* rhodopsin lead to notable structural reorganization and, consequently, to a spectral shift for the absorption band of *L. forbesi* and *A. subulata* rhodopsins. To address this issue, we predicted a three-dimensional model of F270S and S270F mutants of *L. forbesi* and *A. subulata* rhodopsins respectively starting from their amino acid sequences following the protocol described in the "Materials and methods" section.

The analysis of the obtained structures reveals that the F270S substitution causes the structural reorganization of the *L. forbesi* rhodopsin binding pocket including counterion. The distance from the oxygen atom of the counterion E180 to the C15 atom is 5.16 Å (Figure 2d) that is between 6.03 Å and 3.99 Å found for *A. subulata* rhodopsins and *L. forbesi* rhodopsin, respectively. On the contrary, the S270F substitution in the *A. subulata* rhodopsin does not change the distance from the oxygen atom of the counterion E180 to the C15 atom of the chromophore that is 6.01 Å comparing to 6.03 Å (see Figure 2c). Additional analysis of the obtained structures reveals (see Figure 4) that in the *A. subulata* rhodopsin, the M126 residue located in the α-helix III (shown in orange in Figure 4a) is connected by a hydrogen bond network through a water molecule to the S270 residue located in the α-helix VI (shown in green in Figure 4a) and, finally, to the counterion E180, which is located on the relatively flexible β-sheet (shown in red in Figure 4a). For the *L. forbesi* rhodopsin and both studied mutants, M126 does not make a hydrogen bond that is connected the α-helix III and the counterion through the residues of the α-helix VI (Figure 4b). For the *L. forbesi* rhodopsin and the S270F mutant of the *A. subulata* rhodopsin, the F270 residue does not have a part to make a hydrogen bond (Figures 4b, c). For the F270S mutant of the *L. forbesi* rhodopsin, M126 is H-bonded to another residue but not to S270 (Figure 4d). Thus, one of the roles of the S270 residue is an adjustment of the counterion position and, therefore, its distance to the chromophore through an H-bond network.

To summarize, a comparative analysis of the spectral tuning mechanism for the F270S and S270F mutants, *L.*

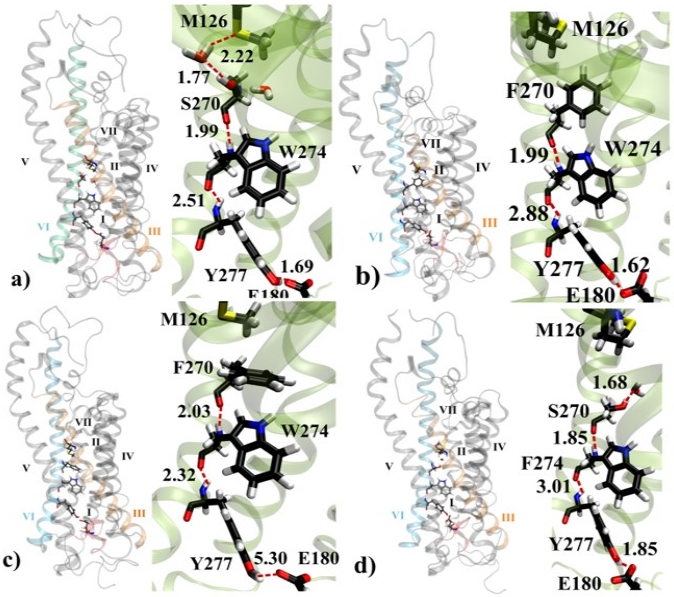

Figure 4 | The differences in hydrogen-bond network that is related to the orientation of E180 counterion in four investigated proteins: visual rhodopsins from *A. subulata* (a), *L. forbesi* (b), *A. subulata* rhodopsin S270F mutant (c) and *L. forbesi* rhodopsin F270S mutant (d). All distances are given in Å. Сравнение сетей водородных связей, которые вызывают реориентацию контриона E180 в четырех изученных белках: зрительных родопсинов *A. subulata* (a), *L. forbesi* (b), мутанта родопсина из *A. subulata* S270F (c) и мутанта родопсина из *L. forbesi* F270S (d). Все расстояния приведены в Å.

tuning mechanism for the F270S and S270F mutants, *L. forbesi* and *A. subulata* rhodopsins shows that the reorganization of the charged and polar residues in the binding pocket, which is caused by F270S substitution, is responsible only for a part of the spectral shift between *L. forbesi* and *A. subulata* rhodopsins. The rest of the spectral shift is due to the reorganization of residues located outside of the binding pocket. According to our models, this reorganization is caused by other substitution/substitutions than F270S. Additional computational/experimental work has to be performed to locate these mutations.

4. Concluding Remarks

In this study we investigated the origin of a spectral shift between visual rhodopsins from two squid species – *A. subulata* and *L. forbesi* that live at different depths in the ocean. To accomplish this task, we constructed a series of QM/MM models for these two rhodopsins, the F270S mutant of *L. forbesi* rhodopsin and the S270F mutant of *A. subulata* rhodopsin. We calculated λ_{max} values for these proteins, and performed an extensive analysis of their spectral tuning mechanisms. We showed that the origin of the 5 nm spectral shift between rhodopsins from *A. subulata* and *L. forbesi* is the consequence of the protein reorganization (non-direct tuning) caused by at least two mutations including S270F rather than an effect of a single specific amino acid substitution. Also, we find that the effect of the S270F substitution cannot be explained by the direct electrostatic effect of polar hydroxyl-bearing serine that replaces non-polar phenylalanine due to its far location from the chromophore.

Generally, these two squid rhodopins provide a striking example of non-direct tuning mechanism. The obtained results can be useful for the rational design of modern rhodopsin-based tools with altered optical properties that can be used in the fields of optogenetics and molecular visualization.[28,29] .

Заключение

В данной работе мы изучили причину спектрального сдвига между зрительными родопсинами двух кальмаров — *A. subulata* и *L. forbesi*, которые живут на различной глубине в океане. Для решения данной задачи мы сгенерировали ряд квантово-механических/молекулярно-механических моделей для этих двух родопсинов, а также мутанта родопсина из *L. forbesi* (F270S), рассчитали для них значения λ_{max} и провели детальный анализ механизмов, отвечающих за их спектральные свойства. Мы показали, что причиной 5 нм спектрального сдвига между родопсинами *A. subulata* и *L. forbesi* является реорганизация белка (непрямая регуляция спектральных свойств), вызванная как минимум двумя мутациями, включая замену S270F, а не определенная одиночная мутация. Также мы показали, что эффект аминокислотной замены S270F не является прямым электростатическим эффектом замены полярного серина, содержащего гидроксильную группу, на неполярный фениланин, так как данная аминокислота находится далеко от хромофора.

Таким образом, изученные родопсины кальмаров представляют собой показательный пример непрямой регуляции спектральных свойств. Полученные результаты могут быть использованы для рационального дизайна современных устройств оптогенетики и молекулярной визуализации на основе родопсинов с модифицированными оптическими свойствами

Acknowledgements

The work was supported by the SPbAU RAS state order, project 16.9790.2017/Bch. The research was carried out using equipment of the shared research facilities of HPC computing resources at the Lomonosov Moscow State University. The research was carried out using computational resources provided by Resource Center “Computer Center of SPbU”. The authors also express their gratitude to the SPbSU Centre for Molecular and Cell Technologies, Magnetic Resonance Research Centre, Chemical Analysis and Materials Research Centre, Centre for Optical and Laser Materials Research.

References

[1] D.M. Hunt, J. Fitzgibbon, S.J. Slobodyanyuk, J.K. Bowmaker, Vis. Res., 36 (1996) 1217-1224.
[2] A. Sivasundar, S.R. Palumbi, J. Evol. Biol., 23 (2010) 1159-1169.
[3] P.A. Jutte, T.W. Cronin, R.L. Caldwell, Mar. Freshw. Behav. Phy., 31 (1998) 231-250.
[4] A. Morris, J.K. Bowmaker, D.M. Hunt, Proc. R. Soc. Lond. B Biol. Sci., 254 (1993) 233-240.
[5] M. Hall, M. Hoon, N. Ryba, J. Pottinger, J. Keen, H. Saibil, J. Findlay, Biochem. J., 274 (1991) 35-40.
[6] M. Murakami, T. Kouyama, Nature, 453 (2008) 363.
[7] M. Stamm, R. Staritzbichler, K. Khafizov, L.R. Forrest, Nucleic Acids Res., 42 (2014) W246-W251.
[8] J. Yang, R. Yan, A. Roy, D. Xu, J. Poisson, Y. Zhang, Nat. Methods, 12 (2015) 7.
[9] A. Morozenko, A. Stuchebrukhov, Proteins, 84 (2016) 1347-1357.
[10] T.J. Dolinsky, P. Czodrowski, H. Li, J.E. Nielsen, J.H. Jensen, G. Klebe, N.A. Baker, Nucleic Acids Res., 35 (2007) W522-W525.
[11] M.H. Olsson, C.R. Søndergaard, M. Rostkowski, J.H. Jensen, J. Chem. Theory Comput., 7 (2011) 525-537.
[12] W.D. Cornell, P. Cieplak, C.I. Bayly, I.R. Gould, K.M. Merz, D.M. Ferguson, D.C. Spellmeyer, T. Fox, J.W. Caldwell, P.A. Kollman, J. Am. Chem. Soc., 117 (1995) 5179-5197.
[13] M. Frisch, G. Trucks, H.B. Schlegel, G.E. Scuseria, M.A. Robb, J.R. Cheeseman, G. Scalmani, V. Barone, B. Mennucci, G. Petersson, in, Gaussian, Inc., Wallingford CT, 2009.
[14] F. Neese, Wiley Interdiscip. Rev. Comput. Mol. Sci., 2 (2012)

73-78.
[15] D.M. Nikolaev, A.A. Shtyrov, M.S. Panov, A. Jamal, O.B. Chakchir, V.A. Kochemirovsky, M. Olivucci, M.N. Ryazantsev, ACS omega, 3 (2018) 7555-7566.
[16] M. Sumita, M.N. Ryazantsev, K. Saito, Phys. Chem. Chem. Phys., 11 (2009) 6406-6414.
[17] A.V. Struts, M.N. Ryazantsev, X. Xu, T.R. Molugu, S.M. Perera, C. Guruge, S. Faylough, C. Nascimento, N. Nesnas, M.F. Brown, Biophys. J., 116 (2019) 204a.
[18] P.Z. El-Khoury, A.N. Tarnovsky, I. Schapiro, M.N. Ryazantsev, M. Olivucci, J. Phys. Chem. A, 113 (2009) 10767-10771.
[19] M.N. Ryazantsev, A. Altun, K. Morokuma, J. Am. Chem. Soc., 134 (2012) 5520-5523.
[20] A. Filatov, N. Knyazev, M. Ryazantsev, V. Suslonov, A. Larina, A. Molchanov, R. Kostikov, V. Boitsov, A. Stepakov, Org. Chem. Front., 5 (2018) 595-605.
[21] D.M. Nikolaev, A. Emelyanov, V.M. Boitsov, M.S. Panov, M.N. Ryazantsev, F1000Research, 6 (2017).
[22] I. Schapiro, M.N. Ryazantsev, W.J. Ding, M.M. Huntress, F. Melaccio, T. Andruniow, M. Olivucci, Aust. J. Chem., 63 (2010) 413-429.
[23] D.S. Parker, B.B. Dangi, R.I. Kaiser, A. Jamal, M. Ryazantsev, K. Morokuma, J. Phys. Chem. A, 118 (2014) 12111-12119.
[24] M.N. Ryazantsev, A. Jamal, S. Maeda, K. Morokuma, Phys. Chem. Chem. Phys., 17 (2015) 27789-27805.
[25] A. Altun, S. Yokoyama, K. Morokuma, J. Phys. Chem. B, 112 (2008) 6814-6827.
[26] A. Altun, S. Yokoyama, K. Morokuma, J. Phys. Chem. B, 112 (2008) 16883-16890.
[27] T. Chan, M. Lee, T. Sakmar, J. Biol. Chem., 267 (1992) 9478-9480.
[28] D.M. Nikolaev, M.S. Panov, A.A. Shtyrov, V.M. Boitsov, S.Y. Vyazmin, O.B. Chakchir, I.P. Yakovlev, M.N. Ryazantsev, in: Progress in Photon Science, Springer, 2019, pp. 139-172.
[29] A.Y. Rotov, L.A. Astakhova, V.S. Sitnikova, A.A. Evdokimov, V.M. Boitsov, M.V. Dubina, M.N. Ryazantsev, M.L. Firsov, Acta naturae, 10 (2018) 75-84.